Rotational Inertia of Nuclei

M. A. Deleplanque, H. J. Körner,[a] H. Kluge,[b] A. O. Macchiavelli,[c] N. Bendjaballah,[d] R. M. Diamond, and F. S. Stephens

Nuclear Science Division, Lawrence Berkeley Laboratory, University of California, Berkeley, California 94720

(Received 13 April 1982)

A new method to determine dynamic effective moments of inertia at high rotational frequencies is presented. The very large values found at the highest spins ($50\hbar$–$55\hbar$) in some Er and Yb nuclei are most likely explained by the alignment of high-j proton orbitals, and could imply triaxial shapes.

PACS numbers: 21.10.Ft, 21.10.Pc

In a rotational nucleus angular momentum is usually generated either by collective rotation or by alignment of single-particle angular momentum along the rotation axis. The competition of these two modes can be studied by measuring different types of moment of inertia.[1] The kinematic moment of inertia,[2] $\Im^{(1)} = I/\omega$, is related to the overall motion of the nucleus. However, $\Im^{(1)}$ does not necessarily describe the response of the system to a torque. That response is related to the differential quantity $dI/d\omega$ which is called a dynamic moment of inertia $\Im^{(2)}$, and is the rate of change in spin with frequency. When there are changes in the internal structure of the nucleus, such as alignment of single-particle angular momentum, I/ω will be different from $dI/d\omega$, reflecting the fact that the nuclear motion is not the simple rotation of a rigid body. These two types of moments of inertia can be defined for any sequence of levels. The collective rotation generates bands, and it is therefore natural to define moments of inertia within a band as $\Im_{\mathrm{band}}^{(2)} = (dI/d\omega)_{\mathrm{band}}$. They can be measured experimentally either from discrete lines or from γ-γ correlation studies.[3] However, a decay path consists of a succession of such bands having different particle alignments. It is then also natural to define effective moments of inertia as $\Im_{\mathrm{eff}}^{(2)} = (dI/d\omega)_{\mathrm{path}}$, which include *both* collective effects *and* particle alignment. $\Im_{\mathrm{band}}^{(2)}$ and $\Im_{\mathrm{eff}}^{(2)}$ are complementary and are the only two moments of inertia presently measurable in the continuum region. Their comparison gives the increase in alignment Δi in a frequency region where the total change of spin is ΔI: $\Delta i/\Delta I = 1 - \Im_{\mathrm{band}}^{(2)}/\Im_{\mathrm{eff}}^{(2)}$. $\Im_{\mathrm{eff}}^{(1)}$, the integral of $\Im_{\mathrm{eff}}^{(2)}$, varies much more smoothly than $\Im_{\mathrm{eff}}^{(2)}$ and is only sensitive to general properties like mass, shape, and pairing correlations.

Both $\Im_{\mathrm{eff}}^{(1)}$ and $\Im_{\mathrm{eff}}^{(2)}$ can be determined from the detection of unresolved (continuum) γ rays emitted after compound-nucleus reactions, in which case they are averaged over many decay paths. The first one has been determined by a "centroid method"[4] from the evolution of the γ-ray spectra obtained in coincidence with slices of increasing total γ-ray energy (spin) detected in a "sum crystal." However, $\Im_{\mathrm{eff}}^{(1)}$ is thereby averaged over a wide range of spins corresponding typically to ~ 50% of the mean entry spin. The value of $\Im_{\mathrm{eff}}^{(2)}$ is related to the height of the γ-ray spectrum (normalized to the γ-ray multiplicity). Since, in a rotational nucleus, the transitions are predominantly stretched $E2$, their number dN is $\approx dI/2$, and the spectrum height H per unit energy interval is $dN/dE_\gamma \approx dI/4d\omega \approx \Im_{\mathrm{eff}}^{(2)}$.[5] In this case $\Im_{\mathrm{eff}}^{(2)}$ is obtained for a spread of frequencies essentially determined by the NaI resolution, which is about 5% in the 0.5-MeV frequency region. But H is a measure of $dI/4d\omega$ only in the frequency region which is fully populated,[4] i.e., up to about 0.35 MeV.

In this Letter, we present a way to correct these spectra for the feeding. It will allow the determination of $\Im_{\mathrm{eff}}^{(2)}$ at frequencies up to about 0.7 MeV in rotational nuclei, higher and with better resolution than previously possible. We take the direct feeding (or feeding curve) corresponding to a certain sum slice to be df/dI, so that the total feeding at spin I_1 is $g(I_1) = \int_{I_1}^{\infty} (df/dI)dI$, normalized to $g(I_1 = 0) = 1 = \int_0^{\infty} (df/dI)dI$. If, on the average, the angular momentum I varies monotonically with frequency (which is true[5] in rotational nuclei), the population above spin I_1 is also above the corresponding frequency ω_1, and the feeding curve in angular momentum corresponds to an average feeding curve in frequency $df/d\omega$, being given by

$$\frac{df}{dI}(I_1) = \frac{df}{d\omega}(\omega_1)\frac{d\omega}{dI}(\omega_1) = \frac{1}{\Im_{\mathrm{eff}}^{(2)}(\omega_1)}\frac{df}{d\omega}(\omega_1).$$

For stretched $E2$ transitions, the spectrum at spin I_1 is $\frac{1}{2}g(I_1)$, and the observed spectrum at ω_1 will be given by $h(\omega_1) = \frac{1}{2}\Im_{\mathrm{eff}}^{(2)}(\omega_1)g(I_1)$

$=H(\omega_1)g(I_1)$. Under the assumption that the next sum slice has a similar feeding pattern, slightly shifted in spin by a "step" ΔI, its observed spectrum is $h_\Delta(\omega_1)=\frac{1}{2}\mathfrak{I}_{\rm eff}^{(2)}(\omega_1)\int_{I_1-\Delta I}^{\infty}(df/dI)dI$, and the difference of these two spectra at a frequency ω_1 is $\Delta h(\omega_1)=\frac{1}{2}\mathfrak{I}_{\rm eff}^{(2)}(\omega_1)\Delta I[df/dI]_{I_1}=\frac{1}{2}\Delta I[df/d\omega]_{\omega_1}$, the feeding curve multiplied by a constant step size ΔI which cancels out in the normalization. Having determined $df/d\omega$ from the difference spectrum $\Delta h(\omega)$ (nonzero between $\omega_{\rm min}$ and $\omega_{\rm max}$), one can correct $h(\omega)$ to obtain the "true" spectrum $H(\omega)$ corresponding to full feeding:

$$H(\omega)=h(\omega)\int_{\omega_{\rm min}}^{\omega_{\rm max}}\frac{df}{d\omega}d\omega\left[\int_{\omega}^{\omega_{\rm max}}\frac{df}{d\omega}d\omega\right]^{-1} \qquad (1)$$

for $\omega_{\rm min}<\omega<\omega_{\rm max}$, and $H(\omega)=h(\omega)$ for $\omega<\omega_{\rm min}$. Typically $\omega_{\rm min}$ is of order 0.35 MeV and $\omega_{\rm max}$ is about 0.8 MeV, so that this method can double the range of frequencies for which $\mathfrak{I}_{\rm eff}^{(2)}$ can be deduced.

The method has been tested with a model program[5] that generates spectra from spin slices similar to the experimental ones (Gaussians with a superimposed spin cutoff), and then treats them exactly like the data. It has been found that the feeding correction is sensitive to (1) the spin step (which should be $\lesssim 10\%$ of the width of the feeding curve) and (2) shape changes in the feeding curve. For conditions approximating the experimental situation, the results are much better if the spectrum corresponding to the lower spin slice is corrected, and the error rarely exceeds 10% for corrections of a factor of 2. It seems likely that this remains true even if the width of the frequency distribution at a given spin becomes comparable to the width of the feeding curve.[6] More details will be presented in a forthcoming paper.

Three different rotational systems have been studied at the 88-in. cyclotron of the Lawrence Berkeley Laboratory: ^{130}Te + ^{40}Ar, ^{126}Te + ^{40}Ar, and ^{124}Sn + ^{40}Ar at 185 MeV. These lead essentially to ^{166,165}Yb, ^{162,161}Yb, and ^{160,159}Er, respectively. The targets were all backed with lead, which stops the beam with very little background and prevents the attenuation of the product angular distributions by hyperfine fields. The total energy was recorded in two 33-cm-diam×20-cm-thick sum crystals whose axes were vertical and centered on the target and whose front faces were 1.9 cm away from the target. The γ-ray spectra were recorded in seven 12.7-cm×15.2-cm NaI detectors in coincidence with the sum crystals. One NaI crystal was at 90° to the beam; the other six were as close as possible to 0° or 180°. A Ge(Li) detector at 90°, also in coincidence with the sum crystals, identified the reaction products for different total γ-ray energies. For each sum slice considered (properly corrected for solid angle), the unfolded γ-ray spectra from all NaI detectors were added and normalized to their multiplicity (measured from the ratio of coincidences to sum-crystal singles). A statistical spectrum of the form $E_\gamma^3\exp(-E_\gamma/T)$, with $T=0.5$ MeV and normalized in the 2.4 to 4 MeV region, was then subtracted. The remaining yrast part of the spectrum was corrected for feeding as outlined above. The experimental 0°/90° ratio was then used to obtain the isotropic corrected spectrum which is directly proportional to $\mathfrak{I}_{\rm eff}^{(2)}$. Pileup effects in the NaI detectors are less than 5% in the frequency region of interest and therefore have been neglected. Examples of both spectra and difference spectra are given in Ref. 4.

Figure 1(a) shows three different $\mathfrak{I}_{\rm eff}^{(2)}$ spectra as a function of frequency for the ^{126}Te + ^{40}Ar system. They correspond to various differences of γ-ray spectra, all with steps of 7% to 8% of their width: Two are deduced from low-spin slices (triangles) and high-spin slices (squares) and the third (circles) covers both ranges. They are in remarkable agreement, although the feeding corrections at a given frequency are quite different for these various spectra. In general, one does not necessarily expect these curves to be identical since the deexcitation pathways might differ, and in fact the curves do differ at low frequencies due to the formation of different product nuclei. In the present cases, the paths followed at higher frequencies are similar enough to give consistent values for different entry spins, and to give confidence in the validity of the method. For corrections up to a factor of 2, the standard deviation of the results is expected to be ~ 10%. Although the data are very consistent for corrections up to a factor of 4, the model calculations show that under a few special conditions, which cannot be excluded experimentally, the errors can become several times larger in this region.

The peaks at 0.22 and 0.26 MeV in Fig. 1(a) are the known discrete lines in the product nuclei ^{162,161}Yb. The first backbend around 0.3 MeV in the even ^{162}Yb nucleus also shows up as a peak since several transitions are piled up near the same frequency. Such an alignment generates a large amount of angular momentum in a small frequency range. The blocked backbend is also

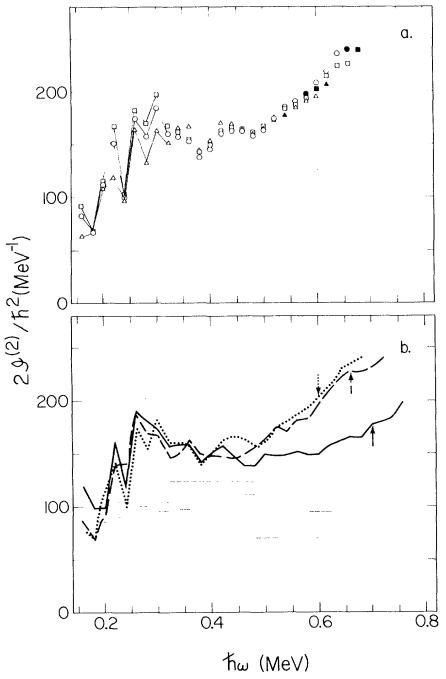

FIG. 1. (a) $\mathfrak{I}_{\rm eff}^{(2)}$ as a function of $\hbar\omega$ for the system ^{126}Te + ^{40}Ar (see text). In each of these plots, the filled symbols show location of 50% and 25% feeding (correction factors of 2 and 4, respectively); spectra are not plotted beyond the 25% feeding point. (b) Average of plots similar to those in (a) for the systems ^{124}Sn + ^{40}Ar (thick solid line), ^{126}Te + ^{40}Ar (dotted line), ^{130}Te + ^{40}Ar (thick dashed line). In each case, the arrow locates the 50% feeding point. Also shown are some values of $\mathfrak{I}_{\rm band}^{(2)}$ for ^{124}Sn + ^{40}Ar (thin solid lines) and ^{130}Te + ^{40}Ar (thin dashed lines).

seen as a small bump around 0.35 MeV.

Beyond the known discrete lines, the most impressive feature in Fig. 1(a) is the large rise of $\mathfrak{I}_{\rm eff}^{(2)}$ starting at a frequency of 0.5 MeV and continuing up to the highest ones measurable around 0.7 MeV. Such an increase is most likely to be produced either by a shape change or by some alignment effects, or both. Fig. 1(b) shows a moment of inertia spectrum for ^{162,161}Yb which is an average of the three curves drawn in Fig. 1(a). It is compared to similar average curves for ^{166,165}Yb and ^{160,159}Er. The behavior of $\mathfrak{I}_{\rm eff}^{(2)}$ is essentially identical at high frequencies for ^{166,165}Yb and ^{162,161}Yb. In ^{160,159}Er, it rises more slowly and only above $\omega = 0.6$ MeV. ^{160}Er and ^{162}Yb, which have the same number of neutrons, behave very differently, whereas the two Yb systems, which differ by 4 neutrons, are similar at high frequencies. This suggests that the protons are playing the more important role, probably

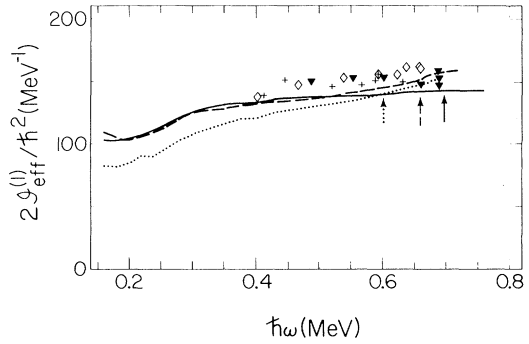

FIG. 2. Plots of $\mathfrak{I}_{\rm eff}^{(1)}$ as a function of $\hbar\omega$, deduced from the centroid method (symbols), and $\mathfrak{I}_{\rm eff}^{(2)}$ integral (lines) for the following systems: ^{124}Sn + ^{40}Ar (inverted triangles, solid line), ^{126}Te + ^{40}Ar (plusses, dotted line), ^{130}Te + ^{40}Ar (diamonds, dashed line).

populating aligned $i_{13/2}$ and $h_{9/2}$ orbitals which are coming down to the Fermi level at these frequencies, as calculated by several groups.[7,8] The thin dashed line shows the collective contribution $\mathfrak{I}_{\rm band}^{(2)}$ in ^{166,165}Yb deduced from the known discrete lines up to $\omega \simeq 0.3$ MeV and from the measured correlation spectra at higher frequencies.[9] The latter $\mathfrak{I}_{\rm band}^{(2)}$ values above 0.5 MeV are somewhat tentative due to the weak valley-ridge structure, but seem to drop at the frequency where $\mathfrak{I}_{\rm eff}^{(2)}$ becomes larger, suggesting that an increasing proportion of the angular momentum is generated by aligning particles. The thin solid line shows $\mathfrak{I}_{\rm band}^{(2)}$ obtained[3] for ^{160,159}Er. It has the same tendency, though to a lesser extent.

The filling of these high-j orbitals could also trigger an increase in deformation or a change of shape. A larger deformation might be expected to favor collective rotation over alignment, whereas the reverse would generally be true for a shift toward triaxial shapes. Thus, the increased alignment discussed above and the lack of strong rotational features (valley and ridges) in the correlation spectra at these frequencies may suggest triaxial shapes. The filling of the $i_{13/2}$ and $h_{9/2}$ proton particle states (in contrast to the previously filled $i_{13/2}$ quasineutron and $h_{11/2}$ quasiprotron orbitals which are mixed *particle-hole* states) would tend to drive the system triaxial.

From the $\mathfrak{I}_{\rm eff}^{(2)}$ values, $\mathfrak{I}_{\rm eff}^{(1)}$ can be calculated:

$$\mathfrak{I}_{\rm eff}^{(1)}(\omega_1) = (1/\omega_1)\int_0^{\omega_1}\mathfrak{I}_{\rm eff}^{(2)}(\omega)d\omega + I_c/\omega_1. \quad (2)$$

This, however, involves estimating the transitions lost below $\omega = 0.15$ MeV (the spectrum cutoff), and some contribution from the statistical

γ rays, and is therefore much less certain in the low-frequency region. These spectra are shown in Fig. 2 for the different systems considered, together with values deduced using the centroid method. Much of the detailed structure of the $\Im_{\rm eff}^{(2)}$ spectrum is lost in the $\Im_{\rm eff}^{(1)}$ spectrum. The increase at low frequencies is due both to the Coriolis antipairing and to the first backbend. The values deduced from the centroid method are systematically higher by 5 to 10%. Part of this can be accounted for by systematic effects in this method due to the narrowing of the difference spectra with increasing spin. It might also be partly associated with temperature effects, since the centroid method always involves the very first transitions emitted, and therefore states at higher temperatures.

The determination of dynamic effective moments of inertia to much higher frequencies provides some new insights into nuclear behavior at very high spins. The observed values at high spins are very large, approaching twice the rigid-sphere value. The evidence suggests that these are due largely to alignment of proton orbitals, probably $i_{13/2}$ and $h_{9/2}$. The observed features would be consistent with increasing triaxiality at these spins ($50\hbar - 55\hbar$) although other possibilities certainly exist.

This work was supported by the Director, Office of Energy Research, Division of Nuclear Physics of the Office of High Energy and Nuclear Physics of the U. S. Department of Energy under Contract No. DE-AC03-76SF00098.

[a]Permanent address: Physik Department, Technische Universität, München, West Germany.
[b]Permanent address: Hahn-Meitner-Institute Berlin, D-1000 Berlin 38, West Germany.
[c]Permanent address: Comisión Nacional de Energía Atómica, Buenos Aires, Argentina.
[d]Permanent address: C.S.T.N., B.P. 1017, Alger, Algeria.

[1]A. Bohr and B. Mottelson, Phys. Scr. 24, 71 (1981).
[2]Except when numerical values are involved, we use units where $\hbar = 1$.
[3]M. A. Deleplanque *et al.*, Phys. Rev. Lett. 45, 172 (1980).
[4]H. J. Körner *et al.*, Phys. Rev. Lett. 43, 490 (1979).
[5]M. A. Deleplanque, I. Y. Lee, F. S. Stephens, R. M. Diamond, and M. M. Aleonard, Phys. Rev. Lett. 40, 629 (1978).
[6]Th. Døssing, private communication.
[7]G. Leander, Y. S. Chen, and B. S. Nilsson, Phys. Scr. 24, 164 (1981).
[8]S. Frauendorf, Phys. Scr. 24, 349 (1981).
[9]M. A. Deleplanque, Phys. Scr. 24, 158 (1981).

Measurement of the ^{7}Be$(p,\gamma)^8$B Reaction Cross Section at Low Energies

B. W. Filippone,[a] A. J. Elwyn, and C. N. Davids
Argonne National Laboratory, Argonne, Illinois 60439

and

D. D. Koetke
Valparaiso University, Valparaiso, Indiana 46383

(Received 4 November 1982)

The absolute total cross section for the reaction ^{7}Be$(p,\gamma)^8$B has been measured for $E_{\rm c.m.} = 117 - 1230$ keV by detecting the delayed α particles following the ^{8}B β decay. Two independent methods have been used to determine the areal density of the ^{7}Be target. The inferred zero-energy S factor from the present experiment is $S_{17}(0) = 0.0216 \pm 0.0025$ keV b. This value reduces the predicted ^{37}Cl solar-neutrino capture rate by ~25%.

PACS numbers: 25.40.Lw, 27.20.+n

In the solar interior ^{8}B is thought to be produced via the reaction ^{7}Be$(p,\gamma)^8$B. The subsequent β decay of this ^{8}B gives a spectrum of neutrinos with $E_\nu = 0$–14 MeV. These neutrinos are expected to provide ~75% of the events in the Brookhaven National Laboratory ^{37}Cl solar-neutrino experiment.[1] The discrepancy between the calculation of the solar-neutrino flux[2,3] and the experiment persists (the so-called solar-neutrino problem). It has been noted recently[2] that a sig-

